ISSN 1061-933X, Colloid Journal, 2007, Vol. 69, No. 4, pp. 411–424. © Pleiades Publishing, Ltd., 2007.
Original Russian Text © M.O. Gallyamov, L.N. Nikitin, A.Yu. Nikolaev, A.N. Obraztsov, V.M. Bouznik, A.R. Khokhlov, 2007, published in Kolloidnyi Zhurnal, 2007, Vol. 69, No. 4, pp. 448–462.

Formation of Superhydrophobic Surfaces by the Deposition of Coatings from Supercritical Carbon Dioxide

M. O. Gallyamov[a], **L. N. Nikitin**[b], **A. Yu. Nikolaev**[b], **A. N. Obraztsov**[a], **V. M. Bouznik**[c], **and A. R. Khokhlov**[c]

[a] *Department of Physics, Lomonosov Moscow State University, Vorob'evy gory, Moscow, 119992 Russia*
[b] *Nesmeyanov Institute of Organoelement Compounds, Russian Academy of Sciences, ul. Vavilova 28, Moscow, 119991 Russia*
[c] *Institute of Physicochemical Problems of Ceramic Materials, Russian Academy of Sciences, ul. Osernaya 48, Moscow, 119361 Russia*

Received October 6, 2006

Abstract—The deposition of uniform coatings of fluorinated polymers from solutions in supercritical carbon dioxide on a number of rough substrates allowed superhydrophobic (ultrahydrophobic) properties to be imparted to their surfaces, and, namely, to increase the value of the contact angle for water droplet to 150° and greater. The dynamics of changing of geometry of a drying droplet on a substrate is studied. A procedure is developed that permits the penetration of water into the substrate to be detected.

DOI: 10.1134/S1061933X07040035

INTRODUCTION

Physical Principles of the Effect of Superhydrophobicity

Superhydrophobic surfaces are characterized by high values of water contact angles (up to 150° o and greater) and a low hysteresis of contact angles (a few degrees). This allows for the easy removal of water droplets from these surfaces, together with particles of possible impurities. Such "self-cleaning" of superhydrophobic surfaces is termed "the lotus effect," as it is analogous to the processes observed in lotus leaves and some other plants [1]. It is known that the maximum contact angle for water on a smooth surface of hydrophobic materials does not exceed 120°. However, it is also known that the macroscopic hydrophobicity of the surface can be substantially enhanced through an increase in its roughness. The superhydrophobic properties of lotus leaves are explained precisely by the combination of nano- and microreliefs of the surface of crystallites of the hydrophobic paraffins that form the outer layer of the leaf.

Two main theoretical models were proposed to describe the interrelations between the hydrophobicity and roughness of the surfaces. The Wenzel model is true at low degrees of roughness [2], while the Cassie–Baxter model is valid at higher roughness [3]. The Wenzel formula makes is possible to describe an increase in the contact angle with increasing surface roughness by the following relation:

$$\cos\tilde{\theta} = r\cos\theta, \qquad (1)$$

where $\tilde{\theta}$ is the contact angle on the rough surface, θ is the contact angle on the smooth surface of the same material, and r is the roughness factor determined by the ratio of the areas of real surface and its geometric projection on the plane. The Cassie–Baxter formula gives an alternative variant for describing an increase in the contact angle on the rough surface compared to the smooth surface as follows:

$$\cos\tilde{\theta} = -1 + \varphi_s(1 + \cos\theta), \qquad (2)$$

where parameter φ_s, determined as the fraction of surface coming into contact with the droplet of the wetting liquid, is introduced in place of the roughness factor. This definition implies that, as the surface roughness increases, the droplet of liquid no longer uniformly wets the surface at a certain moment (i.e., it wets both the local hills and valleys on the surface), but rests on the highest regions of the surface. The first (Wenzel) regime is characterized by the large value of hysteresis of the contact angle, that is, by the droplet sticking to the surface [4, 5]. The mechanism of the transition from Wenzel's to Cassie's regime has been described theoretically [6].

Necessary Conditions for the Appearance of Superhydrophobicity

Thus, in order to produce an ultrahydrophobic surface, it is necessary to satisfy two conditions: (i) the surface should be rough (according to biomimetic approach, with the combination of nano- and microrelief) and (ii) the surface material should by hydrophobic (the water contact angle on a smooth surface should exceed 90°).

The latter condition is necessary for the roughness to precisely increase the hydrophobic properties of a material (otherwise, according to Wenzel formula, we can obtain an "ultrahydrophilic" surface).

This problem can be solved using different approaches. Among these approaches are to increase the roughness of an originally smooth hydrophobic surface, direct formation of the rough surface of the hydrophobic material, deposition of a rough hydrophobic film on an arbitrary (including smooth) substrate, and the hydrophobization of the surface layer of rough (porous) hydrophilic material. In recent years, an abrupt increase in the number of publications devoted to superhydrophobicity (or ultrahydrophobicity) has taken place. In light of the fact that the total number of publications in this field presently run into several hundreds, we did not intend to compile an analytical review for each of the aforementioned approaches. The problem of systematization of studies performed in this field of research has been touched upon in some previously published reviews [7–14].

Hydrophobization of the Surface Layer of Rough or Porous Material

In important practical cases, it often happens that a material with a rough or porous surface prepared in some way does not demonstrate sufficient hydrophobicity. In this case, it becomes possible to induce the superhydrophobic properties through the hydrophobization of the surface layer. The procedure developed in this work is intended to approach this problem. It is worth noting that the possible alternate approaches to this problem include ion plasma treatment (e.g., the treatment of polymers in fluorine-containing plasma), the chemical or plasma chemical deposition of hydrophobizing agents from the vapor phase, and the deposition of various hydrophobic films, including polymer films.

The Application of Supercritical CO_2 as a Solvent to the Deposition of Hydrophobizing Coatings

The method realized by us follows the scheme of the preparation of an superhydrophobic surface through the deposition of a uniform film of hydrophobizing agent from the solution in the supercritical medium, supercritical (SC) carbon dioxide. The supercritical medium is a highly mobile (like a gas) but dense (like a liquid) fluid. Its application as a solvent used to deposit a hydrophobizing coating presents some fundamental advantages compared with the use of traditional liquid solvents. For example, it is very important that the resulting hydrophobized surface potentially accessible for water droplets would be covered with a thin, uniform film of hydrophobic material. If the walls of the deep pores remain unmodified, water vapor can condense inside of them, which evidently leads to the loss of superhydrophobicity of this surface [15–17].

In using a liquid solution of hydrophobizing agent, the problem arises of its penetration into the narrow pores. Indeed, if a liquid solvent poorly wets the substrate to be hydrophobized, the surfaces of deep pores remain unmodified, which does not allow for superhydrophobic properties to be induced in this type of porous structure. On the contrary, if a liquid solvent wets well the modified surface, upon the removal of solvent from the pores, the droplets of drying solution can cause the deposited thin film coating, and even the porous structure itself to fracture due to the capillary forces. The need for only a thin film of hydrophobizing agent to be deposited is a result of the necessity of preserving the morphology of a developed surface. In particular, it is evident that in the hydrophobization of the porous structures of the elements of sensors, membranes, gas-diffusion layers, etc., open pores should remain open to preserve the optimized functional and transport properties of the porous material. These problems can be solved using the proposed procedure for depositing hydrophobizing coatings from SC CO_2.

A number of approaches to the use of supercritical technologies for the deposition of modifying coatings on solid substrates are described in the literature. The procedure for depositing low molecular weight polytetrafluoroethylene and other fluorinated polymers from the vapor phase at 10–200 kPa is patented [18]. The disadvantage of this procedure is its limited applicability, as it can only be used with low molecular weight or oligomeric compounds with sufficient volatility. On the other hand, it is known [19–22] that a number of hydrophobic fluorine- and silicon-containing polymers dissolve in SC CO_2 under laboratory conditions. Therefore, the evident solution of this problem is the deposition of hydrophobic polymers from their solutions in SC CO_2 rather than from the vapor phase.

The two methods that are most widely used for applying SC CO_2 to the formation of thin layer coatings are the method involving the rapid expansion of supercritical solutions or suspensions (RESS) [23–34] and the method involving supercritical antisolvent (SAS) [35–42]. Both methods are based on the use of a solvent–antisolvent pair for a specific polymeric material. In the RESS method, a polymer solution in the SC CO_2 is injected into the gaseous phase through the nozzle where the polymer loses its solubility and is deposited on the substrate surface (thus, the gaseous phase is an antisolvent). On the contrary, in the SAS method, a polymer solution in the ordinary liquid solvent is injected into the SC CO_2, which in this case acts as an antisolvent. In both cases, the morphology of the coating formed is determined by the kinetics of the condensation of polymeric material; as a rule, the coating has nonuniform granular structure. Through the use of these approaches, one can form superhydrophobic coatings on smooth substrates, provided that hydrophobic material is employed. It stands true, however, that, regardless of the numerous examples of the formation of coatings using the RESS or SAS methods, the results of the study of their hydrophobicity are not described in the published literature. However, both approaches cannot be applied when it is necessary to hydrophobize a porous or rough substrate (without distorting its morphology) by depositing a thin, uniform polymer film onto its entire accessible surface.

Thus, it seems promising to use another approach, namely, to use the SC CO_2 as a solvent in the deposition of hydrophobizing polymeric material without the use of an antisolvent (however, with the addition of cosolvents to increase the dissolving power of SC CO_2). This suggests the exposure of the treated surface in a high pressure cell containing a polymer solution in the SC CO_2.

Similar experimental schemes have yielded good results in the deposition of uniform coatings of various technologically promising materials, such as polymers [43–45] and organic compounds [46, 47], as well as organosilicon [48] and organometal [49–51] precursors onto various substrates involving a subsequent reduction to ultrathin metal film or nanoparticles. Data have been published testifying to the prospects of using SC CO_2 as a solvent in formation of self-assembled monolayers characterized by a high level of uniformity [52–56]. However, the utilization of this procedure for depositing coatings from SC CO_2 to enhance the hydrophobicity of substrates has not been described.

Several fundamental advantages of using SC CO_2 as a solvent in forming hydrophobizing thin-film coatings on rough (porous) materials should be emphasized. First, the dissolving power of SC CO_2 substantially depends on temperature and pressure, which makes it possible to experimentally determine and realize the optimal dynamics of the deposition of polymer films with possible control over the thickness of the coating, including in the nanosized range. Second, supercritical fluid, due to its properties, fills the entire available volume (as a gas) and can penetrate into the open pores, on the walls of which the hydrophobizing polymer will be deposited. Third, the liquid CO_2 phase is absent under atmospheric pressure, which excludes the reorganization of the polymer coating deposited onto the surfaces of pores under the action of capillary forces upon the removal of solvent and simultaneously eliminates the problem of residual solvent. Also note the ecological purity and low price of CO_2.

We demonstrated earlier that one can form ultrathin (nanosized thickness) coatings with large degree of uniformity by depositing fluorinated polymer molecules from SC CO_2 onto the atomically smooth surfaces of crystalline substrates of mica and highly oriented pyrolytic graphite [57–62]. A similar approach allows for the deposition of a protective coating of a perfluorinated polymer onto the surfaces of dispersed microparticles, as well as for composite material with a core–shell structure to be obtained [63, 64]. However, coatings deposited onto the aforementioned surfaces were not superhydrophobic due to the absence of the two-level roughness needed to realize the lotus effect. In this work, we used the previously tested approach for the formation of superhydrophobic surfaces characterized by a water contact angle of 150° and larger.

EXPERIMENTAL

Materials

Ultradispersed polytetrafluoroethylene (UPTFE) Forum (Ftor ORganicheskii Ultradispersnyii Material, Institute of Chemistry, Far East Division, Russian Academy of Sciences, Russia) was chosen as the main hydrophobic polymer coating. This commercial material is the product of the thermal gas dynamic destruction of commercial polytetrafluoroethylene and consists of a mixture of low molecular weight and oligomeric perfluorinated linear chains, $(–CF_2–)_n$, with an average number of units, $n \approx 100$. We also used Teflon AF2400 copolymer (DuPont, US), poly(4,5-difluoro-2,2-bistrifluoromethyl-1,3-dioxole-*co*-tetrafluroethylene) with a content of dioxole groups of 87 mol%. For the realization of the RESS method, we used octacosane $C_{28}H_{58}$ (Aldrich).

Various porous and rough materials, such as polymer track-etched membranes, microporous and composite polymer structures, porous woven and nonwoven materials, and nanostructured and crystalline surfaces were tested as substrates. In this work, we only report the results for substrates in which we succeeded in increasing the water contact angles to >130°, i.e., to a value exceeding the maximum attainable magnitude for smooth hydrophobic substrates.

Experimental Unit

High purity CO_2 (OAO Linde Gas Rus, Russia, > 99.997%) was transformed into the supercritical state (temperature above 31.1°C, pressure higher than 7.4 MPa) using a high-pressure unit schematically represented in Fig. 1. The unit consists of reaction cell *1* for the exposure of substrate *2*, liquid thermostat *3* for the stabilization of the temperature regime of exposure, valve system *4*, capillary lines *5* and manometers *6* for the supply of SC CO_2 to the cell, manual pressure generator *7* for the transformation of CO_2 into the supercritical state, and cylinder *8* with CO_2.

Hydrophobization Procedure

The modification of substrates was performed according to the following procedure using hydrophobizing agents. Prior to the experiment, a reaction cell with a volume of 10 ml was carefully and successively washed with various solvents, including SC CO_2 at the final stage. Then, the substrate, subjected to exposure, with an area of about 1 cm^2 and a weighed polymer sample of the requisite mass, was placed into the cell. The polymer sample was preliminarily weighed with an Ohaus AP-250D (Ohaus, US) high precision analytical balance characterized by a standard measurement deviation of about 2×10^{-5} g. In the event of the com-

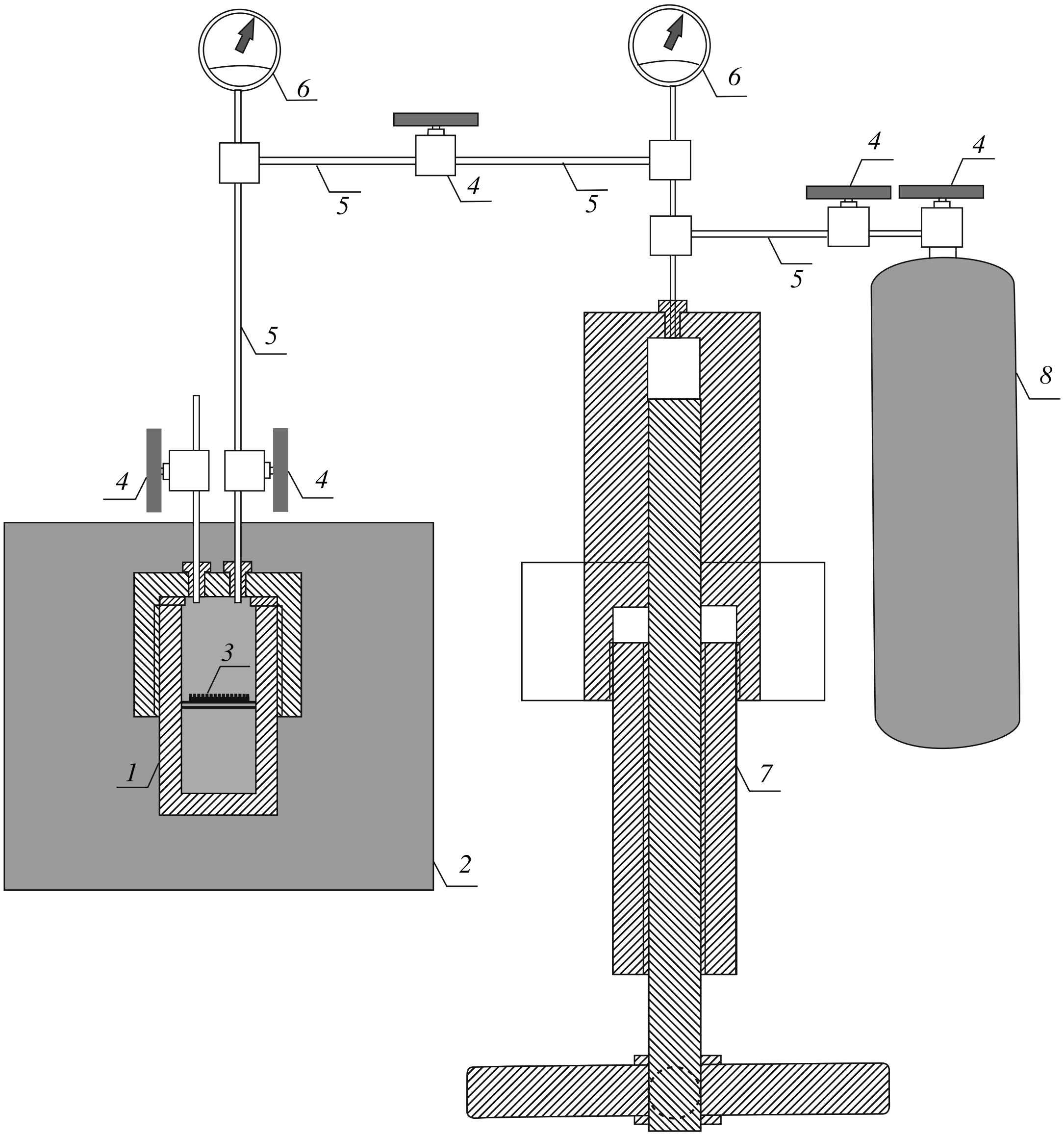

Fig. 1. Scheme of a high pressure unit for the deposition of coatings from solutions in SC CO_2 on the substrate surface. *1*. reaction cell; *2*. liquid thermostat; *3*. exposed substrate; *4*. valves; *5*. capillaries; *6*. manometers; *7*. plunger hand-operated pressure generator; and *8*. cylinder with CO_2.

plete dissolution or dispersion of polymeric material, the concentration of the solution or dispersion was determined by the ratio of the mass of weighed sample to the volume of the cell. The mass of the weighed sample was chosen so that the values of concentration fall on 0.01–0.1 g/l range. The cell was closed, sealed, and blown with CO_2 to remove traces of air and water. Afterwards, the requisite pressure at the given temperature was built up in the cell, which was placed into a liquid thermostat *3* using pressure generator *7* via capillary system *5* equipped with valves *4* and manometers *6* for pressure control. The temperature regime was established throughout the exposure process using an automatic system of temperature maintenance controlled by the thermostat. The sample exposure was performed over 2–4 h followed by cell decompression with CO_2 discharge. During the CO_2 discharge process, the cell temperature was maintained at a level exceeding the critical value of 31.1°C to prevent the formation of liquid CO_2 in the cell. The rate of CO_2 yield was 0.1–1 g/s. At high rates, the cell was cooled to a considerable extent owing to the effect of throttling (which could lead to the undesirable formation of liquid CO_2 phase in the cell, as well as to the condensation of moisture on the supercooled sample after the cell opening). Following decompression, the cell was dismantled and the modified substrate withdrawn; its hydrophobicity was investigated by measuring the contact angle with a Femtoscan Radian setup (Center of Advanced Technologies, Russia).

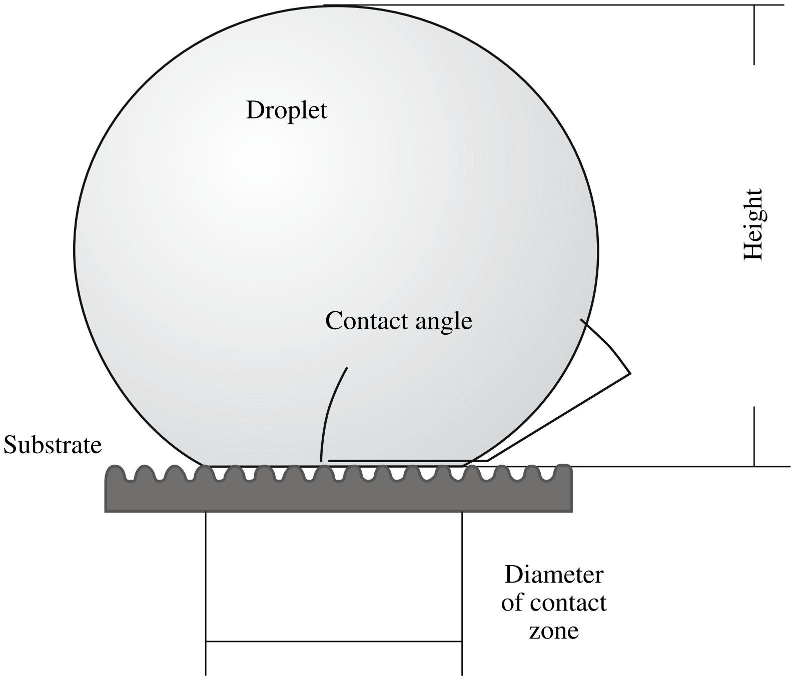

Fig. 2. Measured geometric parameters of the sessile droplet on the substrate, where θ is the contact angle, *h* is the height above the substrate; and *s* is the diameter of the contact zone.

Within the framework of our study, we did not pose the problem of determining the boundaries of the solubility regions for hydrophobizing agents used in the SC CO_2 (the boundary values of temperature and pressure). We only fixed the condition that the total or partial dissolution of a weighed sample of a given polymeric hydrophobizing agent can take place at the chosen experimental parameters (set by the temperature and pressure inside the cell). This was detected based on the absence of the hydrophobizing agent placed on the cell bottom at the onset of experiment after the completion of the sample's exposure, and its reprecipitation on the entire accessible surface area of the inner part of the cell.

The experiments performed demonstrated that superhydrophobicity may be induced in modified surfaces under the following conditions of exposure: at a temperature of 65°C, a pressure of 65 MPa, and an exposure time of 3 h. Decompression should be performed at 40°C at a rate of 0.5 g/s. In most cases, these parameters were used as the standards (designated below as the "standard conditions of exposure"). Slight variations in the temperature, pressure, and time of exposure, as well as in the temperature and rate of decompression around the aforementioned values within 10°C, 10 MPa, 1 h, and 0.1–1 g/s, respectively, did not noticeably affect the obtained numerical characteristics of the degree of superhydrophobicity (the measured values of the water contact angle).

It was found, however, that at lower temperature and pressure values, the solubility of polymeric hydrophobizing agents in SC CO_2 decreases. At lower decompression temperatures, CO_2 is transformed into a liquid state and its removal is accompanied by the negative effects of capillary forces on the deposited structures. At higher rates of decompression, the cell is overcooled due to the throttling effect, which can lead to the formation of liquid, or even solid, CO_2 in the cell, as well as potentially distorting the morphology of the deposited coatings.

Procedure for Measuring Contact Angles

A droplet of test liquid (water) with a volume of several microliters was placed on the substrate surface and the dynamics of its geometry measured over 1000 s (17 min) with a digital camera. In doing so, we measured the time dependences of the following geometric parameters of the droplet: the height *h* above the substrate, the diameter *s* of the contact zone with the substrate, and the contact angle θ using adapted software (see Fig. 2).

Assuming the spherical geometry of a droplet, the value of the contact angle can be calculated independently from the measured values of *h* and *s* and using the relation

$$\theta' = \begin{cases} \arcsin\left(\dfrac{sh}{s^2/4 + h^2}\right) & h < s/2 \\ \pi - \arcsin\left(\dfrac{sh}{s^2/4 + h^2}\right) & h > s/2, \end{cases} \tag{3}$$

derived via elementary geometric analysis.

According to our analysis, θ and θ' begin to differ at large absolute values of contact angles, a feature which is explained by the deformation of the droplet and the deviation of its shape from a spherical one. The differences in θ and θ' values can be as large as 10°. The violation of the applicability of the spherical droplet model means that the calculated values of the geometric contact angle θ' are underestimated. However, in some cases, it was difficult to directly measure contact angle θ (e.g., due to unclear droplet boundaries or excessive roughness of the substrate, which blocks any visual inspection of the contact zone). Therefore, during our analysis, we used the averaged value of contact angle

$$\theta'' = \frac{\theta + \theta'}{2},$$

taking into account that the thus calculated value of the contact angle can be underestimated by several degrees; however, we assume that this does not distort the general tendency of its variations with time.

The measured geometric parameters of the droplet allow for the surface area, S_a, of its contact with the substrate to be calculated as follows:

$$S_a = \pi s^2/4, \tag{4}$$

while droplet volume V (in the approximation of its spherical geometry) is calculated as follows:

$$V = \pi h^3\left(\frac{s}{2h\sin\theta} - \frac{1}{3}\right). \tag{5}$$

The time dependences of the above-mentioned measured and calculated values were analyzed.

The droplet volume decreases with time due to evaporation. However, along with the evaporation through the free surface, the liquid can penetrate from the droplet into the porous substrate through the contact zone. This type of penetration serves as an indicator of insufficient superhydrophobicity (water ultrarepellency) of a substrate. The penetration of moisture into the porous substrate considerably decreases the value of the contact angle and increases its hysteresis. It is expected that the deposition of a thin, uniform polymer coating onto the entire open pore surface should prevent the penetration and condensation of moisture in the porous structure. Thus, the evaluation of the sorption behavior of a substrate with respect to the droplet resting on its surface yields additional important information on the quality of the hydrophobization of rough substrate, the mechanical stability of the coating, and its influence on the porous structure of the substrate and therefore can act as a criterion in the comparative analysis of the characteristics of materials obtained.

Thus, it was necessary to develop a procedure allowing for the separation of the contributions of two mechanisms to the decrease in the droplet volume – due to the evaporation or penetration of water into the porous structure of substrate. Two main scenarios of the variations in the geometry of sessile droplet are observed in the experiments.

Scenario I—the contact angle does not change with time; the area of the contact zone and the droplet volume decrease monotonically, which, in combination with the droplet evaporation, corresponds to the absence of the hysteresis of the contact angle.

Scenario II—the contact angle decreases monotonically with time to a certain value; in this case, the area of the contact zone remains constant, whereas the droplet volume also decreases, which, in combination with droplet evaporation, corresponds to the presence of the hysteresis of contact angle. The hysteresis of the contact angle can indirectly testify to the penetration of moisture into the porous or rough structure, and should be taken into account when analyzing the results.

Transient cases can take place occasionally in which it is difficult to attribute the tendency observed to either scenario I or II with full certainty.

Taking into account the presence of the two main scenarios mentioned above, we analyzed the problem of droplet evaporation through the free surface. The solution of this problem makes it possible to differentiate the contributions of evaporation and sorption to the decrease in the volume by comparing the dynamics of the variations in volume of the two droplets, for which the reference droplet rests on a nonsorbing substrate and the testing droplet resides on a potentially sorbing substrate under identical experimental conditions.

If it is assumed that flux J of water evaporating from the droplet surface is determined only by the difference between the current value of the partial pressure of water vapor and the pressure of saturated water vapor (this allows for J to be considered a parameter of the problem), then the decrease in volume V of the spherical droplet due to the evaporation through the free surfaces is described by the formula

$$\rho\frac{dV}{dt} = -JS, \tag{6}$$

where ρ is the density of a liquid. Taking into account the known formulas for the volume and surface area of a sphere, this differential equation is reduced to the equation for the radius r of the droplet,

$$\frac{dr}{dt} = -\frac{J}{\rho},$$

the solution of which, being linear relative to time, makes it possible, taking into account the initial condition (the initial droplet volume is V_0), to derive the following formula that describes the change of volume in the droplet due to evaporation with time:

$$V(t) = V_0\left(1 - \frac{t}{\tau}\right)^3, \tag{7}$$

where characteristic parameter τ, with the dimension of time, is defined by the formula

$$\tau = \left(\frac{3}{4\pi}\right)^{1/3} \frac{\rho V_0^{1/3}}{J}.$$

Model dependence (6) is true for the case of the evaporation of a spherical droplet under the assumption that flux J is independent of the presence of a substrate, and, that the degree of vapor saturation near the droplet is determined by external conditions only (the evaporation in well-stirred atmosphere when the rate of evaporation is low compared to the rate of vapor diffusion in the environment).

The real problem of the evaporation of a droplet resting on a substrate surface is more complex, particularly due to the fact that three time dependent unknown variables are present in Eq. (6), namely, height h above the substrate, diameter s of the contact zone, and contact angle θ (see Eqs. (4) and (5)).

However, the use of evident trigonometric relations allows one of the unknown variables to be expressed through the other two. Furthermore, taking into account the observation mentioned above, we can, in most of the cases of the two main experimental scenarios, make a simplifying assumption based on the constant values of the contact angle θ (scenario I) or diameter s of the contact zone with time (scenario II). This enables us to reduce the differential equation describing the process of droplet evaporation to an equation with respect to one unknown time-depending function that permits the integration. It turned out that, in the first case (constant contact angle and the absence of hysteresis, scenario I), the droplet height decreases linearly with time, while the variations of a volume with time are described by a type (7) equation. The analytical expression for time constant τ is slightly cumbersome and includes trigonometric functions of θ, which, in view of the constancy of the latter parameter, can be considered only as additional numerical multipliers. In the second case (of a constant diameter of the contact zone and the presence of distinct wetting hysteresis, scenario II), the search for an analytical expression is complicated (see [65]). In transient cases, when the behavior of the droplet on the substrate combines the main features of scenarios I and II, the analysis of the experimental dependences using analytical solutions becomes even more complicated.

Therefore, we used another approach, for which we analyzed the obtained dependences using numerical methods. In fact, by knowing the current values of the geometric parameters of a droplet at each moment, we can calculate the current value of its free surface by the formula

$$S' = \frac{\pi h s}{\sin\theta}. \tag{8}$$

Then, upon the partition of the temporal evolution of volume of the droplet, $V(t)$, into small time intervals during which the S' value can be considered constant, the following approximation of a small decrease in volume over current time interval Δt is true:

$$V(t_1) = V(t_{i-1}) - \frac{J}{\rho} S'(t_{i-1})\Delta t, \tag{9}$$

which, evidently, is the finite difference expression of Eq. (6). The numerical approximation of experimental dependences $V(t)$ by finite difference (9) and the search for the best approximation coefficient J/ρ allows the evaporation flux J to be found, which is determined by experimental conditions (relative humidity). The evaporation flux can be considered constant for all droplets, provided that the conditions are identical (in the approximation that the evaporation process is independent of the presence of the substrate). This makes it possible to perform the reference measurements of the rates of droplet evaporation from the surfaces of definitely nonsorbing substrates (crystals; waterproof polymers, e.g., polytetrafluoroethylene; etc.). In this case, approximating experimental dependences $V(t)$ by finite difference (9), we can determine evaporation flux J and use the value obtained to analyze the decrease in the volume of droplets on rough substrates that are potentially capable of sorbing. This type of analysis enables us to conclude whether the dynamics of a decrease in the volume of a droplet on a rough surface is described exclusively by evaporation, and, if it is not, to determine to what extent the sorption of moisture by the substrate contributes to this decrease. Naturally, the problem of creating rough, water-ultrarepellent surfaces requires the minimization of the penetration of moisture into the substrate; hence, a such an analysis makes it possible to judge the quality of the hydrophobized surface.

Additional indirect information on this fact is often given by the value of the contact angle hysteresis as follows: large hysteresis evidences some penetration of water into a porous or rough substrate, and/or of the reorganization of its structure in the zone of contact with the droplet. Therefore, small contact angle hysteresis is a necessary property of an superhydrophobic, water-repellent surface. Indeed, large values of contact angle hysteresis imply that the poor wettability of substrate is a temporary phenomenon when there is a contact of its surface with water or a humid atmosphere; the wettability will be enhanced with the penetration of moisture into the substrate. Consequently, this type of surface cannot be considered truly superhydrophobic.

According to the published data, wetting hysteresis is traditionally determined experimentally by measuring the difference between the advancing and receding contact angles by the alternate increase or decrease of the droplet volume (using, for example, a microsyringe). We revealed that contact angle hysteresis often

Results of the observations of the changes in the geometry of sessile droplets of water on the surfaces of substrates studied in the course of evaporation and results of the analysis of the penetration of liquid into the porous structure of substrate. For the classification of scenarios see text

Substrate	Contact angle, deg		Surface area of the contact zone, cm^2		Water penetration into the porous substrate	Scenario
	immediately after droplet deposition	at a 50% decrease in droplet volume	immediately after droplet deposition	at 50%-decrease in droplet volume		
Paper	84	50	0.075	0.075	present	II
Paper with UPTFE coating	150	141	0.0095	0.0098	none present	II
Nanostructured graphite substrate	153	143	0.015	0.015	present	II
Nanostructured graphite substrate with a UPTFE coating	158	154	0.009	0.007	none present	I
Mica	0	–	–	–	–	–
Mica with an octacosane coating	150	142	0.0088	0.0083	none present	I, II
Carbon fabric	119	50	0.032	0.065	present	II
Carbon fabric with a Teflon AF2400 coating	133	116	0.022	0.024	none present	II

depends on the duration of contact between the droplet and the substrate; moreover, this dependence is particularly large at small values of contact time. Therefore, we discarded the traditional procedure for directly determining the wetting hysteresis and instead evaluated only the hysteresis based on the total decrease in the contact angle of a droplet that was in contact with the substrate for a long period of time. Because the rate of droplet evaporation was determined by the current experimental conditions, the initial moment and corresponding to 50% decrease in volume of the sessile droplet due to its evaporation were chosen as reference parameters. We used this type of evaluation for the comparative analysis of various hydrophobized substrates. In practice, the presence of contact angle hysteresis leads to the sticking of a droplet to the wetted region of a surface, while the surface area of the contact zone remains unchanged until the contact angle decreases to the value corresponding to the receding angle. A pronounced wetting hysteresis may result from the fracturing of the coating in the contact zone and, in this case, acts as an indicator of the stability of the deposited coatings.

RESULTS AND DISCUSSION

The Modification of Paper by the Deposition of UPTFE Coating

The problem of a uniform, profound hydrophobization of a paper surface has an important applied significance due to the demand for similar technology in the polygraphic industry, the production of photographic materials, etc. Therefore, it was of interest to us to apply the procedure for preparing uniform coating made of UPTFE Forum grade deposited from the SC CO_2 onto surface of paper having porous structure, as well as to study its wettability by water.

The surface modification of paper (Canon, office grade) was performed by depositing UPTFE from the SC CO_2 under standard conditions (see above). The results of the observations of water droplets on the surfaces of initial and hydrophobized papers are shown in Figs. 3a and 4, and are summarized in the table. These data evidence that the water droplets behave according to scenario II described above (the presence of pronounced wetting hysteresis): the area of the contact zone remains unchanged with evaporation throughout the observation time and the contact angle decreases monotonically. After the deposition of hydrophobic UPTFE coating from SC CO_2, the paper surface demonstrates superhydrophobic properties (the initial contact angle is ~150°). The comparison of the dynamics of the variations in droplet volumes on the surfaces of an initial (unmodified) sample of paper and nonsorbing material (PTFE) made it possible to conclude that the decrease detected in droplet volume is explained by both the evaporation of water and its penetration into the porous substrate. The results of a similar analysis of the samples of paper exposed to the SC CO_2 containing hydrophobizing agent demonstrated the absence of a detectable contribution to the decrease in droplet volume due to the sorption of water by the porous substrate.

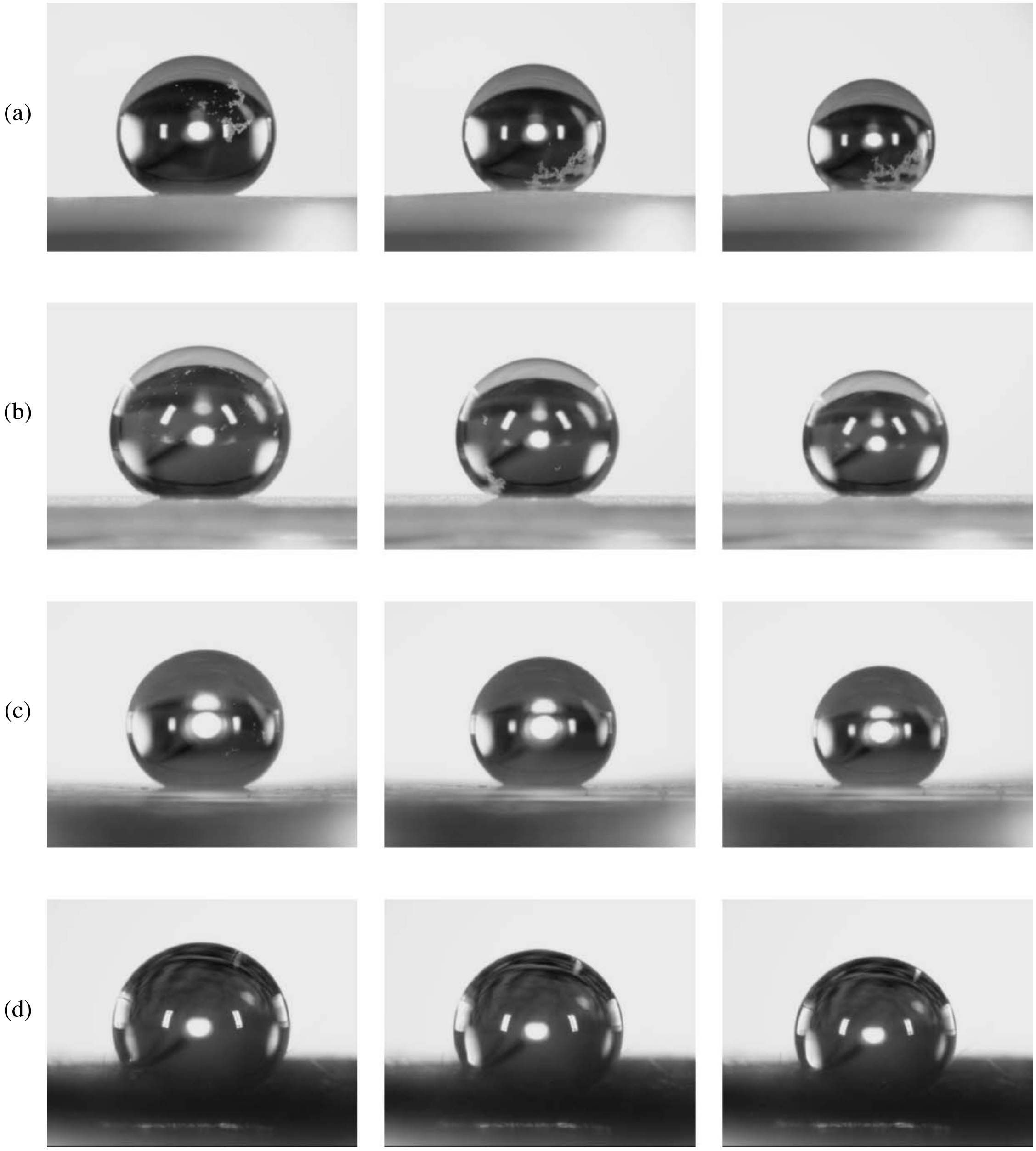

Fig. 3. Dynamics of the variations in the geometry of water droplets on different surfaces: (a) paper with UPTFE coating, (b) nanographite with UPTFE coating, (c) mica with octacosane coating, and (d) carbon fabric with Teflon AF2400 coating. From right to left: immediately after deposition at 500 and 1000 s after; Frame size 4.4 × 3.5 mm^2.

Significant wetting hysteresis observed for both modified and initial papers makes it possible to suggest that the substrate structure changes in the contact zone with the test droplet of water and the penetration of water into a porous structure take place in both cases (although it is not always detected experimentally). This is indirectly evidenced by a visually observed local swelling of the paper surface near the contact zone even for the sample modified by the deposition of the coating made from UPRFE. Apparently, this may result from the insufficient mechanical stability of a hydrophobic coating made from this material on the surface of this porous substrate.

Modification of Rough Carbon Materials by the Deposition of a UPRFE Coating

Porous and rough carbon materials, being the components of filters, sorbents, gas diffusion layers, and electrodes, are widely used in industry, including in high technology. The important problem to be solved in many specific applications is the deposition of thin, uniform, functional polymeric coating e.g., (hydrophobic)

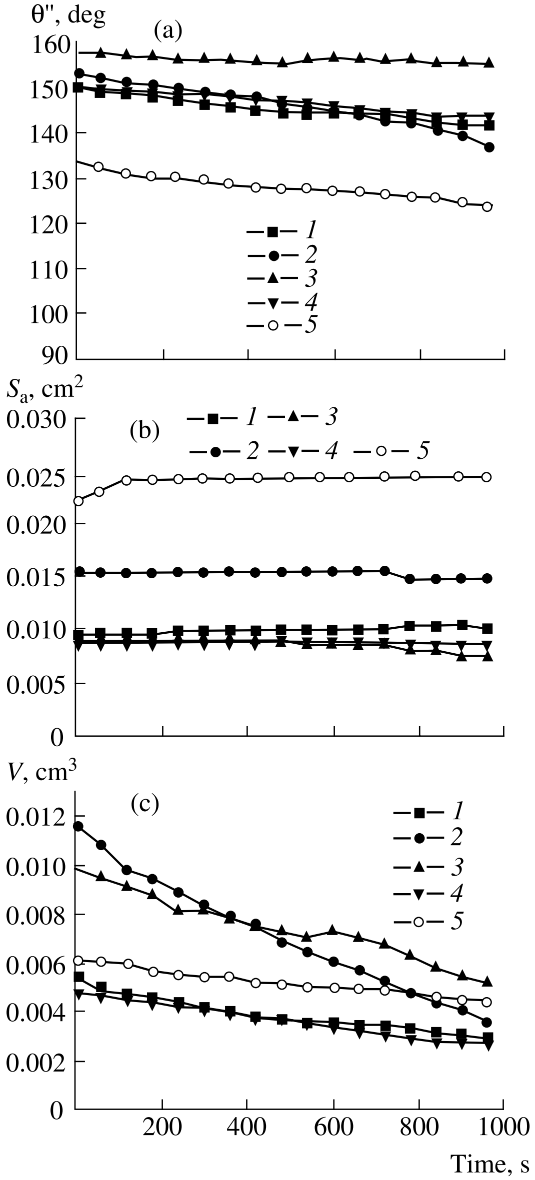

Fig. 4. Dynamics of the variations with time in the (a) contact angle θ'', (b) surface area of contact site S_a, and (c) volume of water droplets on (1) paper with UPTFE coating, (2) initial nanographite, (3) nanographite with UPTFE coating, (4) mica with octacosane coating, and (5) carbon fabric with Teflon AF2400 coating.

onto the accessible surface of porous carbon material. In this case, the coating should not change the morphology and properties of a material (the porosity and the pore size distribution).

In connection with this, it seems interesting to apply the procedure for depositing uniform fluorine-containing coating from SC CO_2 onto the surface of porous carbon nanomaterial (nanographite) prepared by plasma chemical synthesis from the gaseous phase. This material is a carbon film deposited onto the surface of silicon wafer and consists of nanosized crystallites of graphite [66, 67].

The results of the study of the water wetting of initial graphite and graphite hydrophobized by depositing UPTFE from SC CO_2 are shown in Figs. 3b and 4, and in the table. It can be seen from these results that water droplets on surfaces of initial nanographite demonstrate behavior close to that preset in scenario II (the presence of a pronounced hysteresis of the contact angle), whereas after the deposition of the hydrophobic coating, the behavior is close to scenario I (the absence of significant hysteresis).

Both of the surfaces of initial nanographite and of that modified by the deposition of UPTFE display superhydrophobic properties (contact angle > 150°) at the initial stage of contact with the water droplet. The dynamics of the change in droplet volume was studied on a surface of porous nanographite in the initial state, as well as after the UPTFE coating was deposited, and, as a reference, on a smooth surface of pyrolytic graphite. A comparison of results obtained under identical experimental conditions for the surfaces of initial nanographite and nonsorbing pyrolytic graphite has made it possible to conclude that the detected decrease in droplet volume is explained by both the evaporation of moisture and its penetration into the porous structure of unmodified nanographite. No moisture penetration into the porous structure was revealed for the substrate made of nanographite with a UPTFE coating deposited.

Furthermore, the data obtained allows direct calculation of water loss due to sorption by the porous nanographite substrate. For this purpose, using numerical analysis by Eq. (9), we first determined typical values of evaporation flux for a water droplet of the same volume placed on a surface of nonsorbing pyrolytic graphite under the current experimental conditions (air humidity and temperature). The obtained value of evaporation flux was then used to approximate the losses due to evaporation in the testing droplet on a surface of porous nanographite. Following this, the difference between the experimentally observed losses and those due to evaporation will determine the sorption losses, being looked for. A plot of the calculated dependence of these losses on time is presented in Fig. 5. An estimate of the average sorption flux per surface area S_a of the contact between the droplet and substrate yields a value of $J \approx 2 \times 10^{-4}$ g/(cm^2 s). This value exceeds the analogous value obtained for the sorption flux through the contact zone for a droplet resting on a paper substrate (see above) by approximately one order of magnitude. Thus, the parent nanographite is characterized by a large initial value of water contact angle, and, at the same time, by high sorbability relative to water. Thus, in this case, we can only speak of the "apparent," or "temporal," water repellency, which gradually vanishes upon the contact of the substrate with moisture. Indeed, as the porous structure of the substrate is flooded by water, the water contact angle should logically be lowered. It is precisely this fact that explains experimentally observed considerable wetting hysteresis, in which the value of the contact angle decreases monotonically with a decrease in droplet volume, whereas the area of the contact zone remains almost unchanged. It can be assumed that the porous structure of the substrate is flooded by water in the contact zone and that the droplet of water sticks to the surface.

Thus, we are able to draw an important conclusion from the experimental data that large initial values of the contact angle and small initial values of contact angle hysteresis are insufficient to attribute one or another surface to a class of hydrophobic surfaces. In order to substantiate this conclusion, it is necessary to investigate the dynamics of the variations of water repellency over a period of sufficiently long contact between the substrate and testing droplet. According to the published data, it seems that a clear understanding of this phenomenon is lacking, due to the fact that, in some cases, the conclusion about the superhydrophobicity of any substrate is made based only on measurements of the initial values of advancing and receding contact angles.

The modification of a nanographite surface by the deposition of a UPTFE coating prevents the sorption of water by the substrate (a detected decrease in droplet volume is explained only by loss due to evaporation). Thus, the nanographite surface with a deposited UPTFE coating can be considered truly superhydrophobic, as it is characterized by high values of water contact angles and low wetting hysteresis, as well as by the absence of water sorption by the porous structure of the substrate.

The Modification of Smooth Substrates by the Deposition of Hydrophobic Octacosane Coatings

The induction of superhydrophobic properties to smooth substrates requires, not only the uniform hydrophobization of their surfaces, but also the imparting to some degree of roughness to this surface for the realization of the lotus effect. One of the procedures for increasing roughness of a hydrophobic coating deposited onto a smooth substrate involves the spontaneous crystallization of the deposited material. The prospect of such an approach is determined by its universal application to the spontaneous formation of a rough structure; it is not necessary to use structured substrates for the preparation of superhydrophobic materials. In this case, it is possible to impart superhydrophobic properties to any material, including structureless (smooth) substrates.

To elaborate the approach based on this effect, we tested the model system prepared by the deposition of coating from octacosane onto atomically smooth crystalline substrates made of mica and pyrolytic graphite under the standard conditions described above. However, following this approach, we did not succeed in imparting superhydrophobic properties to the substrates; instead, the initial values of water contact angles were 120° and 20° for modified surfaces of pyrolytic graphite and mica, respectively (60° and 0° for the initial surfaces, respectively).

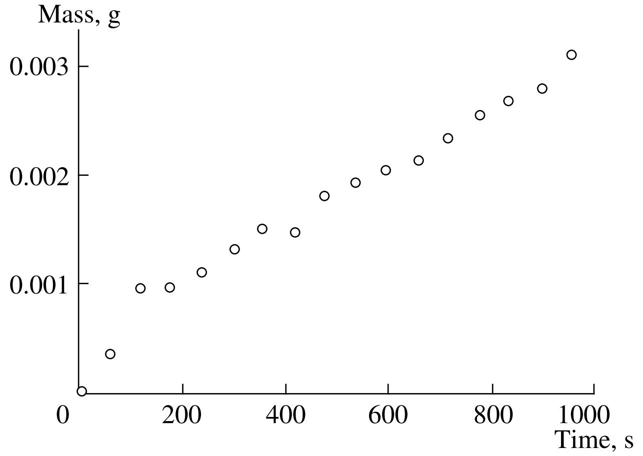

Fig. 5. Sorption of water by the porous nanographite substrate in the region of its contact with the sessile droplet. The time dependence of the mass of sorbed water is shown.

Therefore, in the next series of experiments, the octacosane coating was applied onto the mica surface according to the RESS method described above. (The solubility of paraffins with comparable molecular masses in the SC CO_2 has been studied earlier [68–71].) According to this method, the surface subjected to modification was exposed to a jet of a solution of octacosane in SC CO_2 flowing out of the nozzle of reaction cell. In expanding the SC CO_2 flow coming out of the nozzle, SC CO_2 is transformed into the gaseous state, while octacosane loses its solubility and is condensed on the accessible sites, including on the substrate surface, thus forming a rather stable coating of a substantial thickness. Despite the wide application of the RESS method in the practice of supercritical technologies, there are no examples of its use in producing ultrahydrophobic surfaces.

It turned out that the RESS method can be successfully employed to form superhydrophobic coatings on originally hydrophilic (water contact angle is 0°) atomically smooth mica surface. The corresponding results are shown in Figs. 3c and 4, and are also summarized in the table.

The water contact angle reaches 150° after the deposition of an octacosane coating onto the mica. Upon the evaporation of the water droplet, the surface area of its contact with the substrate decreases slightly, however, only to an extent that insufficiently compensates for the contact angle hysteresis. Thus, the dynamics observed in the droplet is an intermediate one between scenarios I and II and is, apparently, explained by the partial filling of the pores of the octacosane coating

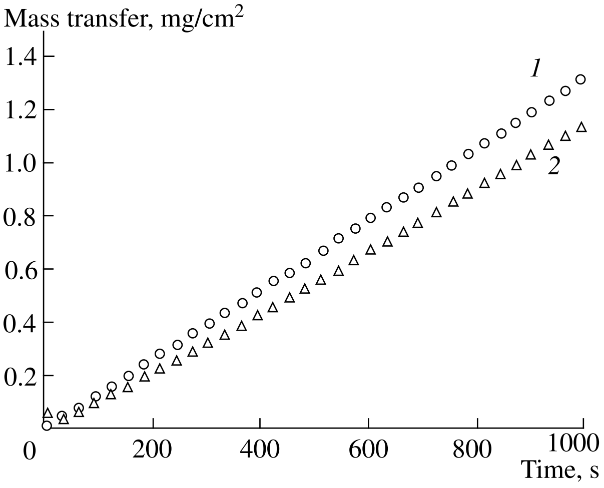

Fig. 6. Transport of water vapor through permeable woven materials: (*1*) initial S-CCG5 carbon fabric and (*2*) fabric modified by the deposition of hydrophobic Teflon AF2400 coating.

with water (the Wenzel regime with sticking, see formula (1)).

Modification of Woven Materials by the Deposition of UPTFE and Teflon AF 2400 Coatings

Uniform and extensive hydrophobization of fabrics is an important task, not only for the textile industry, but also for solving a wider scope of problems, including the production technology of various separating and filtering systems, as well as for biomedical applications involving functional elastic woven materials with controlled specific permeability.

We performed the hydrophobization of a number of woven materials, including an S-CCG5 conducting carbon fabric produced by a SAATI group (Italy) under standard conditions using a Teflon AF 2400 copolymer. The production company positioned this fabric as a component of gas diffusion layers for he cases where the combination of low density, high electronic conductivity, elasticity, and compressibility is necessary in a material. The results of the study of this material are shown in Figs. 3d and 4, and are also summarized in the table. It turned out that the developed approach enables one to increase the hydrophobicity of carbon fabric and prevent the sorption of liquid water (in the absence of a coating, the fiber imbibes the water).

To elucidate how the deposited hydrophobic coating affected the transport properties of woven materials relative to water vapor, we employed the simplest procedure, analogous to the known technological “cup” method. In this method, a vessel containing volatile liquid (water) is closed with a membrane made from testing material and the kinetics of the loss of liquid mass is measured by gravimetry. After some time, the dependence of the mass loss on time reaches the linear asymptotics, whose angle of inclination allows one to estimate the transport characteristics of liquid molecules in a given membrane (the tangent of the slope determines the permeability of the membrane).

It was revealed through the use of this procedure that hydrophobized woven material with a blocked transport of liquid water (see table) preserved its high permeability with respect to water vapor. This is evidenced by the time dependences of the loss of mass (normalized to the unit surface area of the membrane) in the samples of initial S-CCG5 carbon fabric and in the samples modified with Teflon AF2400 (Fig. 6). The experiments were performed under the same conditions regarding temperature and relative humidity. It is seen that hydrophobization only slightly lowers the transport characteristics of water vapor in the fabric, due primarily to the possible blocking of surface diffusion in its pores.

The possibility of preserving the morphology of the substrate porous structure and the free transport of water vapor in the substrate with full blocking of sorption and transport of liquid water due to induced surface superhydrophobicity is particularly important in using woven materials as separators, filters, gas-distributing layers, and breathing hydrophobic (water-repellent) materials. Note that the problem of preventing the flooding of the porous carbon structure with liquid water with the retention of the unimpeded transport of its vapor is an important task in creating gas-diffusion layers of fuel cells. This problem has traditionally been solved by depositing PTFE from dispersions, which requires a considerable amount of a hydrophobizing agent, the deposition of which partially blocks gas transport. The deposition of more uniform coatings with smaller thicknesses is an important technological problem, which can be solved by the use of the approach we have developed.

CONCLUSIONS

A method for producing superhydrophobic surfaces is proposed. The method consists of depositing hydrophobizing coatings from solutions in supercritical carbon dioxide onto a rough or porous substrate. This method was used to hydrophobize a number of model surfaces whose wetting (before and after the deposition of coatings) was studied by analyzing variations in the geometry of sessile droplet of water on the testing substrate. This made it possible to monitor the decrease in the effect of hydrophobicity in the extended contact between the substrate and sessile droplet, to estimate the wetting hysteresis, and to detect the sorption of a liquid by the porous substrate.

It was established that the developed method of hydrophobization allows for ultrahydrophobic and water-ultrarepellent properties to be imparted to paper and nanostructured carbon materials. In addition, we succeeded in developing superhydrophobic coatings on atomically smooth substrates.

The problem of increasing the stability and performance of coatings formed using SC CO_2 requires additional study. A possible procedure for increasing the mechanical stability of coatings is the use of organofluoric compounds that are soluble in SC CO_2 and capable of forming strong chemical bonds with the substrate surface due to special anchor groups that are present in their molecules. In connection with this we can follow the paradigm outlined in [72].

We believe that further elaboration of the tested method can enable the development of specific procedures for imparting superhydrophobic properties to rough, porous, or other substrates with complex surface geometry. In particular, this method can be employed for optimizing the parameters of the gas diffusion layers of the membrane electrode blocks of fuel cells, gas sensors, and adsorbents, including those used for chromatographic columns, filters, instruments for microjet techniques, and print heads of jet printers; for an increase in the biocompatibility of transplants, catheters, and contact lenses; for creating self-cleaning surfaces and surfaces with lower resistance to water flow; for the grease protection of optical lenses, instrumentation for micro- or nanosystems, micro- or nanoelctronic, micromechanic, microelectromechanic, and optoelectronic instruments; for the moisture protection of gunpowder particles and other combustible and explosive materials; for imparting water-repellent properties to fabrics, paper, and other materials; for protecting surfaces from drizzle and moisture condensation and the effects of aggressive media; and for creating thin antifriction coatings for details and machinery.

ACKNOWLEDGMENTS

This study was performed by the State Contract no. 02.442.11.7490 (code 2006-RI-19.0/001/224) within the framework of Federal Target-oriented Program "Research and Innovations in Priority Trends of Scientific and Technical Development for 2002–2006."

REFERENCES

1. Barthlott, W. and Neinhuis, C., *Planta*, 1997, vol. 202, p. 1.
2. Wenzel, R.N., *Ind. Eng. Chem.*, 1936, vol. 28, p. 988.
3. Cassie, A.B.D. and Baxter, S., *Trans. Faraday Soc.*, 1944, vol. 40, p. 546.
4. Quéré, D., Lafuma, A., and Bico, J., *Nanotecnology*, 2003, vol. 14, p. 1109.
5. McHale, G., Shirtcliffe, N.J., and Newton, M.I., *Langmuir*, 2004, vol. 20, p. 10146.
6. Johnson, R.E. and Dettre, R.U., *Adv. Chem. Ser.*, 1964, no. 43.
7. Nakajima, A., Hashimoto, K., and Watanabe, T., *Monatsh. Chem.*, 2001, vol. 132, p. 31.
8. Feng, L., Li, S., Li, Y., et al., *Adv. Mater.* (Weinheim, Fed. Repub. Ger.), 2002, vol. 14, p. 1857.
9. Quéré, D., *Nature Mater.*, 2002, vol. 1, p. 14.
10. Blossey, R., *Nature Mater.*, 2003, vol. 2, p. 301.
11. Gould, P., *Mater. Today,* 2003, vol. 6, no. 11, p. 44.
12. Otten, A. and Herminghaus, S., *Langmuir*, 2004, vol. 20, p. 2405.
13. Sun, T., Feng, L., Gao, X., and Jiang, L., *Acc. Chem. Res.*, 2005, vol. 38, p. 644.
14. Quéré, D., *Rep. Prog. Phys.*, 2005, vol. 68, p. 2495.
15. Lafuma, A. and Quéré, D., *Nature Mater.*, 2003, vol. 2, p. 457.
16. Cheng, Y.-T. and Rodak, D.E., *Appl. Phys. Lett.*, 2005, vol. 86, p. 144101.
17. Wier, K.A. and McCarthy, T.J., *Langmuir*, 2006, vol. 22, p. 2433.
18. Sugimoto, H. and Ohashi, M. Jpn. Patent 11116278, 1999.
19. McHugh, M.A., Mertdogan, C.A., DiNoia, T.P., et al., *Macromolecules*, 1998, vol. 31, p. 2252.
20. Henon, F.E., Camaiti, M., Burke, A., et al., *J. Supercrit. Fluids*, 1999, vol. 15, p. 173.
21. Rindfleisch, F., DiNoia, T.P., and McHugh, M.A., *J. Phys. Chem.*, 1996, vol. 100, p. 15581.
22. Kirby, C.F. and McHugh, M.A., *Chem. Rev.*, 1999, vol. 99, p. 565.
23. Petersen, R.C., Matson, D.W., and Smith, R.D., *J. Am. Chem. Soc.*, 1986, vol. 108, p. 2100.
24. Matson, D.W., Fulton, J.L., Petersen, R.C., and Smith, R.D., *Ind. Eng. Chem. Res.*, 1987, vol. 26, p. 2298.
25. Kim, J.-H., Paxton, T.E., and Tomasko, D.L., *Biotechnol. Prog.*, 1996, vol. 12, p. 650.
26. Shim, J.-J., Yates, M.Z., and Johnston, K.P., *Ind. Eng. Chem. Res.*, 1999, vol. 38, p. 3655.
27. Tepper, G. and Levit, N., *Ind. Eng. Chem. Res.*, 2000, vol. 39, p. 4445.
28. Chernyak, Y., Henon, F., Harris, R.B., et al., *Ind. Eng. Chem. Res.*, 2001, vol. 40, p. 6118.
29. Matsuyama, K., Mishima, K., Umemoto, H., and Yamaguchi, S., *Environ. Sci. Technol.*, 2001, vol. 35, p. 4149.
30. Wang, T.-J., Tsutsumi, A., Hasegawa, H., and Mineo, T., *Powder Technol.*, 2001, vol. 118, p. 229.
31. Wang, Y., Wei, D., Dave, R., et al., *Powder Technol.*, 2002, vol. 127, p. 32.
32. Levit, N., Pestov, D., and Tepper, G., *Sens. Actuators, B*, 2002, vol. 82, p. 241.
33. Fulton, J.L., Deverman, G.S., Yonker, C.R., et al., *Polymer*, 2003, vol. 44, p. 3627.
34. Inoue, H., Jpn. Patent 2001314810, 2001.
35. Mawson, S., Johnston, K.P., Betts, D.E., et al., *Macromolecules*, 1997, vol. 30, p. 71.
36. Reverchon, E., *J. Supercrit. Fluids*, 1999, vol. 15, p. 1.
37. Elvassore, N., Bertucco, A., and Caliceti, P., *Ind. Eng. Chem. Res.*, 2001, vol. 40, p. 795.
38. Chattopadhyay, P. and Gupta, R.B., *Ind. Eng. Chem. Res.*, 2000, vol. 39, p. 2281.
39. Chattopadhyay, P. and Gupta, R.B., *Ind. Eng. Chem. Res.*, 2001, vol. 40, p. 3530.

40. Chattopadhyay, P. and Gupta, R.B., *Ind. Eng. Chem. Res.*, 2002, vol. 41, p. 6049.
41. Chattopadhyay, P. and Gupta, R.B., *Ind. Eng. Chem. Res.*, 2003, vol. 42, p. 465.
42. Wang, Y., Dave, R.N., and Pfetter, R., *J. Supercrit. Fluids*, 2004, vol. 28, p. 85.
43. Glebov, E.M., Yuan, L., Krishtopa, L.G., et al., *Ind. Eng. Chem. Res.*, 2001, vol. 40, p. 4058.
44. Hoggan, E.N., Flowers, D., Carbonell, R.G., and DeSimone, J.M., *Ind. Eng. Chem. Res.*, 2004, vol. 43, p. 2113.
45. Cho, D., Kim, Y.J., Erkey, C., and Koberstein, J.T., *Macromolecules*, 2005, vol. 38, p. 1829.
46. Kim, J., Novick, B.J., DeSimone, J.M., and Carbonell, R.G., *Langmuir*, 2006, vol. 22, p. 642.
47. Kim, J. and Carbonell, R.G., *Langmuir*, 2006, vol. 22, p. 2117.
48. Fukushima, Y. and Wakayama, H., *J. Phys. Chem., B*, 1999, vol. 103, p. 3062.
49. Watkins, J.J., Blackburn, J.M., and McCarthy, T.J., *Chem. Mater.*, 1999, vol. 11, p. 213.
50. Ye, X.R., Wai, C.M., Zhang, D., et al., *Chem. Mater.*, 2003, vol. 15, p. 83.
51. Cabanas, A., Shan, X., and Watkins, J.J., *Chem. Mater.*, 2003, vol. 15, p. 2910.
52. Weinstein, R.D., Yan, D., and Jennings, G.K., *Ind. Eng. Chem. Res.*, 2001, vol. 40, p. 2046.
53. Zemanian, T.S., Fryxell, G.E., Liu, J., et al., *Langmuir*, 2001, vol. 17, p. 8172.
54. Efimenko, K., Novick, B., Carbonell, R.G., et al., *Langmuir*, 2002, vol. 18, p. 6170.
55. Yan, D., Jennings, G.K., and Weinstein, R.D., *Ind. Eng. Chem. Res.*, 2002, vol. 41, p. 4528.
56. Luscombe, C.K., Li, H.-W., Huck, W.T.S., and Holmes, A.B., *Langmuir*, 2003, vol. 19, p. 5273.
57. Gallyamov, M.O., Vinokur, R.A., Nikitin, L.N., et al., *Phys. Low-Dimens. Struct.*, 2002, vols. 5–6, p. 153.
58. Gallyamov, M.O., Vinokur, R.A., Nikitin, L.N., et al., *Langmuir*, 2002, vol. 18, p. 6928.
59. Gallyamov, M.O., Yaminskii, I.V., Khokhlov, A.R., et al., *Mikrosist. Tekh.*, 2003, no. 1, p. 31.
60. Gallyamov, M.O., Yaminskii, I.V., Khokhlov, A.R., et al., *Mikrosist. Tekh.*, 2003, no. 2, p. 11.
61. Gallyamov, M.O., Bouznik, V.M., Tsvetnikov, A.K., et al., *Khim. Fiz.*, 2004, vol. 23, no. 6, p. 76.
62. Shumilkina, N.A., Myakushev, V.D., Tatarinova, E.A., et al., *Vysokomol. Soedin., Ser. A*, 2006, vol. 48, p. 2102.
63. Gallyamov, M.O., Bouznik, V.M., Tsvetnikov, A.K., et al., *Dokl. Akad. Nauk*, 2003, vol. 392, p. 77.
64. Gallyamov, M.O., Bouznik, V.M., Tsvetnikov, A.K., et al., Polym. Prepr. (Am. Chem. Soc., Div. Polym. Chem.), 2004, vol. 45, p. 504.
65. McHale, G., Aqil, S., Shirtcliffe, N.J., et al., *Langmuir*, 2005, vol. 21, p. 11053.
66. Obraztsov, A.N., Zolotukhin, A.A., Ustinov, A.O., et al., *Carbon*, 2003, vol. 41, p. 836.
67. Zolotukhin, A.A., Obraztsov, A.N., Ustinov, A.O., and Volkov, A.P., *Zh. Eksp. Teor. Fiz.*, 2003, vol. 124, p. 1291.
68. McHugh, M.A., Seckner, A.J., and Yogan, Th.J., *Ind. Eng. Chem. Fundam.*, 1984, vol. 23, p. 493.
69. Yau, J.-S. and Tsai, F.-N., *J. Chem. Eng. Data*, 1993, vol. 38, p. 171.
70. Reverchon, E., Russo, P., and Stassi, A., *J. Chem. Eng. Data*, 1993, vol. 38, p. 458.
71. Chandler, K., Pouillot, F.L.L., and Eckert, C.A., *J. Chem. Eng. Data*, 1996, vol. 41, p. 6.
72. Muidinov, M.R., *Ross. Khim. Zh.*, 2002, vol. 46, no. 3, p. 64.